AIP | The Journal of Chemical Physics

Multiplet-specific shape resonance and autoionization effects in (2+1) resonance enhanced multiphoton ionization of O_2 via the d $^1\Pi_g$ state

J. A. Stephens, M. Braunstein, and V. McKoy

Citation: The Journal of Chemical Physics **92**, 5319 (1990); doi: 10.1063/1.458511
View online: http://dx.doi.org/10.1063/1.458511
View Table of Contents: http://scitation.aip.org/content/aip/journal/jcp/92/9?ver=pdfcov
Published by the AIP Publishing

Multiplet-specific shape resonance and autoionization effects in (2+1) resonance enhanced multiphoton ionization of O_2 via the $d\,^1\Pi_g$ state

J. A. Stephens, M. Braunstein, and V. McKoy
Arthur Amos Noyes Laboratory of Chemical Physics,[a] *California Institute of Technology, Pasadena, California 91125*

(Received 9 August 1989; accepted 26 January 1990)

In this paper we discuss the single-photon ionization dynamics of the $d\,^1\Pi_g$ Rydberg state of O_2. Comparision is made with vibrationally resolved measurements of photoelectron spectra which employ (2 + 1) resonance enhanced multiphoton ionization (REMPI) through the $d\,^1\Pi_g$ state. A σ_u shape resonance near the ionization threshold leads to non-Franck–Condon vibrational branching ratios and a substantial dependence of photoelectron angular distributions on the vibrational state of the $X\,^2\Pi_g$ ion. Significant differences exist between our one-electron predictions and experiment. These are mainly attributed to electronic autoionization of repulsive $^1\Sigma_u^-$, $^1\Sigma_u^+$, and $^1\Delta_u$ states associated with the $1\pi_u^3 1\pi_g^3$ configuration. A proposed singlet "K" $^1\Pi_u$ Rydberg state converging to the $A\,^2\Pi_u$ ion probably also contributes to autoionization in the $d\,^1\Pi_g$ state spectrum. We also show that autoionizing H and $J\,^3\Pi_u$ Rydberg states of O_2 converging to the $a\,^4\Pi_u$ and $A\,^2\Pi_u$ ionic thresholds, respectively, may play a previously unsuspected role in the $C\,^3\Pi_g$ state one-color REMPI spectra. We discuss multiplet-specific (spin-dependent) effects via comparision of these results with recent experimental and theoretical studies of $O_2\,C\,^3\Pi_g$ photoionization.

I. INTRODUCTION

The photoionization dynamics of the $C\,^3\Pi_g$ ($1\pi_g 3s\sigma_g$) Rydberg state of O_2 have recently been studied experimentally and theoretically by (2 + 1) resonance enhanced multiphoton ionization spectroscopy (REMPI).[1–5] These studies have shown that a σ_u shape resonance leads to strong non-Franck–Condon ionic vibrational distributions and photoelectron angular distributions. Presently there is significant interest in using REMPI to prepare molecular ions in vibrationally (and rotationally) state-selected states. Since the shape resonance in O_2 was shown to effectively inhibit efficient vibrational state-specific production of ions via the $C\,^3\Pi_g$ state, additional experimental studies have probed the higher-lying "$4s$–$3d$" Rydberg states.[6,7] Due to the symmetry of the excited orbital, some of these levels may not access the σ_u ionization continuum, thus permitting O_2^+ state preparation to better than ~80% for several vibrational levels.

In this paper, we present studies of photoionization dynamics of the $d\,^1\Pi_g$ ($1\pi_g 3s\sigma_g$) Rydberg state of O_2, the singlet analog of the $C\,^3\Pi_g$ state. The $d\,^1\Pi_g$ state of O_2 has been detected, and partially characterized, by several electron impact and REMPI studies.[8–13] The singlet coupling of the $3s\sigma_g$ Rydberg electron to the $X\,^2\Pi_g$ ion core results in a small, positive energy shift of the potential energy curve, relative to the triplet state (~0.1 eV). In contrast, the σ_u shape resonance with its localized character, as well as the energetically accessible valence autoionizing states, exhibit large (~1–3 eV) energy shifts relative to their triplet analogs. Due to these considerations, the REMPI photoelectron dynamics may significantly depend on which spin state of the neutral Rydberg level is accessed in the two-photon absorption step. In particular, the photoelectron spectra observed by Miller *et al.*[14] for the $d\,^1\Pi_g$ Rydberg state display greater non-Franck–Condon behavior than that observed for the $C\,^3\Pi_g$ spectra. As discussed below, we attribute this mainly to autoionization of repulsive valence states and Rydberg states converging to excited states of the ion and not to the σ_u shape resonance. Such multiplet-specific shape resonance and autoionization effects are generally energy dependent. They could be further probed to great advantage via two-color REMPI experiments.

Although we believe that autoionization is the major source of disagreement between present theory and available experiments, another class of electronic interactions relevant to excited-state photoionization dynamics are avoided crossings between the resonantly prepared Rydberg state and repulsive valence states of the same electronic symmetry. Van der Zande *et al.*[15,16] have recently studied the $C\,^3\Pi_g$ and $d\,^1\Pi_g$ Rydberg states of O_2 using charge-exchange translational spectroscopy. Specifically they investigated and deduced details of the Rydberg-valence interactions and associated predissociation processes. These interactions may influence ion vibrational distributions through electronic correlations and perturbations of vibrational levels of the neutral Rydberg in the vicinity of the curve crossing.

In Sec. II we give a brief discussion of numerical details of the calculations. In Sec. III we present vibrational branching ratios and discuss the shape-resonance and electron correlation effects relevant to ionic vibrational distributions for photoionization of the $d\,^1\Pi_g$ Rydberg state. A qualitative discussion of the correlation effects in terms of Franck–Condon factors, survival factors, and SCF calculations is given. Rigorous incorporation of these states in the photoionization calculations remains a major goal of our studies. Also presented in Sec. III are two-color (energy-dependent)

[a] Contribution No. 8015.

branching ratios and vibrationally resolved photoelectron angular distributions. Section IV gives a brief conclusion.

II. CALCULATIONAL DETAILS

In the frozen-core Hartree–Fock approximation there are four dipole-allowed channels for ionization of the $d\,^1\Pi_g$ state corresponding to photoionization of the singly occupied $3s\sigma_g$ Rydberg orbital. The electronic continuum wave functions are

$$\Psi(^1\Pi_u) = \frac{1}{\sqrt{2}}\{|[\mathrm{core}]1\pi_g^+\,\overline{k\sigma_u}| - |[\mathrm{core}]\,\overline{1\pi_g^+}\,k\sigma_u|\}, \tag{1a}$$

$$\Psi(^1\Sigma_u^+) = \tfrac{1}{2}\{|[\mathrm{core}]1\pi_g^+\,\overline{k\pi_u^-}| + |[\mathrm{core}]1\pi_g^-\,\overline{k\pi_u^+}| - |[\mathrm{core}]\,\overline{1\pi_g^+}\,k\pi_u^-| - |[\mathrm{core}]\,\overline{1\pi_g^-}\,k\pi_u^+|\}, \tag{1b}$$

$$\Psi(^1\Sigma_u^-) = \tfrac{1}{2}\{|[\mathrm{core}]1\pi_g^+\,\overline{k\pi_u^-}| - |[\mathrm{core}]1\pi_g^-\,\overline{k\pi_u^+}| - |[\mathrm{core}]\,\overline{1\pi_g^+}\,k\pi_u^-| + |[\mathrm{core}]\,\overline{1\pi_g^-}\,k\pi_u^+|\}, \tag{1c}$$

$$\Psi(^1\Delta_u) = \frac{1}{\sqrt{2}}\{|[\mathrm{core}]1\pi_g^+\,\overline{k\pi_u^+}| - |[\mathrm{core}]\,\overline{1\pi_g^+}\,k\pi_u^+|\}, \tag{1d}$$

where $[\mathrm{core}] = 1\sigma_g^2 1\sigma_u^2 2\sigma_g^2 2\sigma_u^2 3\sigma_g^2 1\pi_u^4$. The associated one-particle Schrödinger equations for the continuum orbitals can be derived straightforwardly[17,18] and have been presented in detail in Eq. (2) of Ref. 5 for the case of triplet coupling. The singlet-coupled equations can be obtained simply by changing the signs preceeding the exchange operators for the $1\pi_g$ electron, and the nonlocal S' terms.

The Gaussian basis sets, internuclear distances, partial-wave expansions, and radial grids used to evaluate the R-dependent transition moments for the $k\sigma_u$ and $k\pi_u$ channels are identical to those for the $C\,^3\Pi_g$ calculations.[3,5] The initial state $d\,^1\Pi_g$ SCF wave functions were calculated using a $(9s5p2d/4s3p2d)$ Gaussian basis set with diffuse functions on the center of mass with exponents identical to those in Ref. 5. The total SCF energy of the $d\,^1\Pi_g$ state at $R = 2.282a_0$ with this basis is $-149.285\,87$ a.u., resulting in an energy splitting of 0.073 eV compared to the $C\,^3\Pi_g$

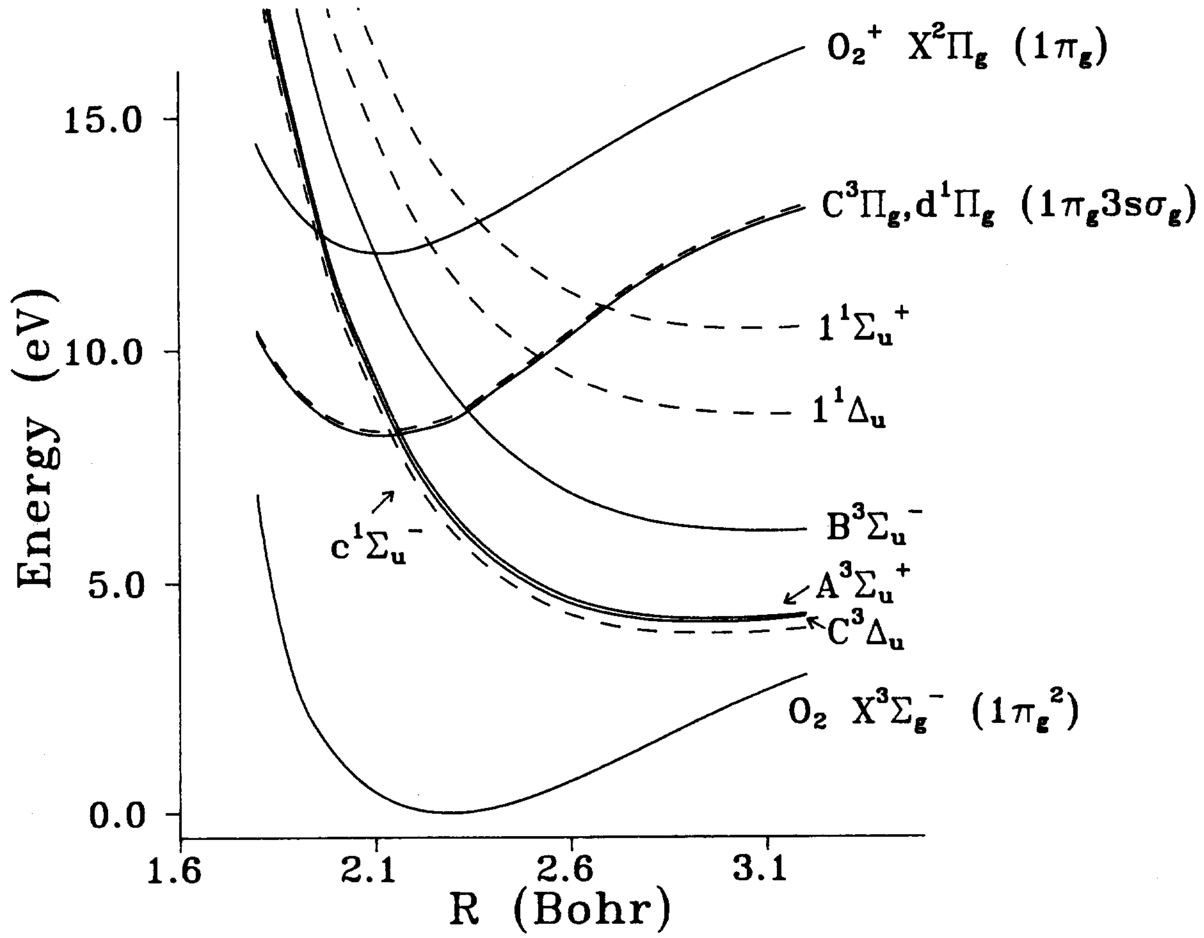

FIG. 1. O_2 potential energy curves for the ground state, the first ionic state, and singlet and triplet valence states deriving from the electronic configuration $1\pi_u^3 1\pi_g^3$. The potential curves are taken from Refs. 29 and 30.

state. The $d\,^1\Pi_g$ state vibrational wave functions and those for the $X\,^2\Pi_g$ ion were calculated using the RKR potentials discussed in Refs. 3 and 5. For later discussion, in Fig. 1 we summarize potential energy curves for the O_2 neutral and ionic ground states and several singlet and triplet Rydberg and repulsive valence states relevant to this discussion.

III. DISCUSSION OF RESULTS

A. Shape resonance effects

In Fig. 2 we show the calculated photoionization cross section for the singlet and triplet-coupled $3s\sigma_g \rightarrow k\sigma_u$ channel at the internuclear distance $R = 2.088\ a_0$. The σ_u shape resonance in the singlet-coupled channel is shifted $\sim$2.5 eV higher in kinetic energy than the triplet-coupled channel, similar to singlet–triplet energy shifts typically observed for excited valence states. This shift is due to the greater (repulsive) exchange interaction of the ionized electron with the ion core in the singlet-coupled final state. In Fig. 2 the large difference between the length and velocity cross sections at low energy is due to our neglect of electron correlations beyond the Hartree–Fock level in the $^{1,3}\Pi_u$ ionization channels. These differences largely cancel upon forming the vibrational branching ratios (see Fig. 3). Residual discrepancies with experiment are attributed mainly to autoionization of repulsive valence states (discussed below).

For ground state photoionization of O_2, the σ_u shape resonance has been discussed by Raseev *et al.*[19] for the $3\sigma_g$ level, and by Gerwer *et al.*,[20] Dittman *et al.*,[21] and Braunstein and McKoy[22,23] for both the $3\sigma_g$ and $1\pi_g$ levels. Particularly for the $3\sigma_g$ level, it was shown[23] that it is essential to include multiplet-specific aspects of this problem to account for observed one-electron features of the photoionization spectra. In these ground and the present excited-state studies, the R dependence of the transition moment induced by the shape resonance results in non-Franck–Condon effects observable in both vibrational branching ratios and photoelectron angular distributions.[24–26]

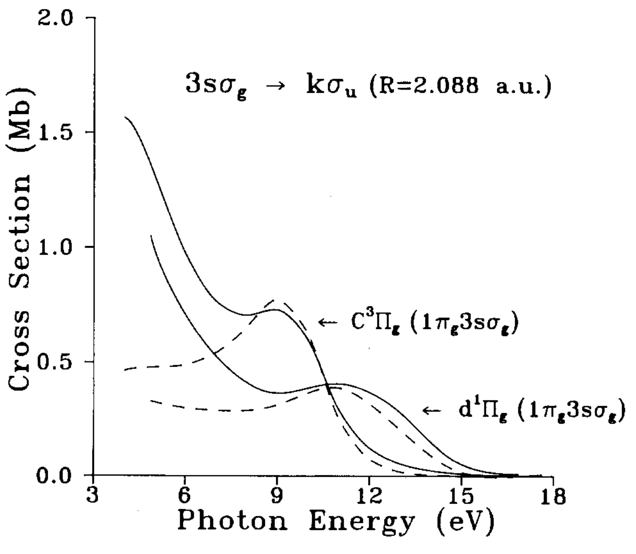

FIG. 2. Calculated photoionization cross sections for the $3s\sigma_g \rightarrow k\sigma_u$ channel of the $O_2\ d\,^1\Pi_g$ and $C\,^3\Pi_g$ states. Solid curves: length form; dash curve: velocity form.

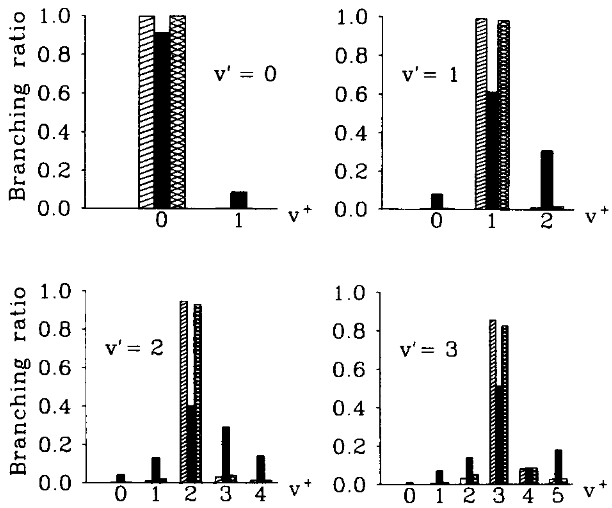

FIG. 3. Calculated vibrational branching ratios for photoionization of the $v' = 0$–3 levels of the $O_2\ d\,^1\Pi_g$ state. Length form (crossed bar); velocity form (crosshatched bar). The calculations are compared with the measurements of Miller *et al.* (Ref. 14, solid bar).

For the present REMPI studies, the shift of the resonance to higher kinetic energy will result in some decrease in the calculated non-Franck–Condon effect, but not as much as Fig. 2 may suggest. Note that the shift in the σ_u resonance position is much larger than the difference in ionization thresholds (3.84 and 3.93 eV for the $v' = 0$ levels, respectively). The photoelectron energies for the $d\,^1\Pi_g$ and $C\,^3\Pi_g$ $(2+1)$ spectra range from $\sim$0.2–1.3 eV, which is a small portion of the abcissa scale in Fig. 2. The σ_u cross section still depends strongly on R, causing only a weak detuning effect when compared against the triplet results.[3,5] Branching ratios and angular distributions which illustrate the energy dependence over a broad energy range are discussed below.

TABLE I. Summary of vibrationally resolved cross sections and branching ratios.

		σ_{v',v^+} (Mb)		$\sigma_{v',v^+}/\Sigma_{v^+}\sigma_{v',v^+}$		$\sigma_{v',v^+}/\Sigma_{v^+}\sigma_{v',v^+}$
v'	v^+	Length (Theory)	Velocity	Length (Theory)	Velocity	(Experiment[a])
0	0	2.8373	0.9946	0.9985	0.9969	0.91
0	1	0.0042	0.0031	0.0015	0.0031	0.089
1	0	0.0050	0.0045	0.0016	0.0042	0.079
1	1	3.0365	1.0489	0.9882	0.9804	0.61
1	2	0.0313	0.0165	0.0102	0.0154	0.31
2	0	0.0073	0.0030	0.0022	0.0025	0.043
2	1	0.0350	0.0241	0.0107	0.0203	0.13
2	2	3.1049	1.1031	0.9450	0.9267	0.40
2	3	0.0971	0.0449	0.0295	0.0377	0.29
2	4	0.0415	0.0152	0.0126	0.0128	0.14
3	0	0.0014	0.0001	0.0004	0.0001	0.012
3	1	0.0216	0.0135	0.0063	0.0103	0.072
3	2	0.1080	0.0694	0.0315	0.0529	0.14
3	3	2.9231	1.0805	0.8535	0.8235	0.51
3	4	0.2802	0.1123	0.0818	0.0856	0.087
3	5	0.0905	0.0363	0.0264	0.0277	0.18

[a] From Ref. 14.

B. Branching ratios and correlation effects

Figure 3 shows our calculated vibrational branching ratios compared with the photoelectron intensities measured by Miller *et al.*[14] for the $v'=0$–3 levels of the $d\,^1\Pi_g$ state. Table I gives a summary of the calculated and measured branching ratios. These distributions have been normalized so that the sum over v^+ for each intermediate level equals unity. Inclusion of the R dependence of the transition moment arising from the shape resonance accounts for some of the observed $\Delta v \neq 0$ intensity, e.g., the $v^+=3$–5 states accessed via the $v'=2$ and 3 intermediate states. The Franck–Condon approximation predicts essentially zero intensity for these off-diagonal transitions. However, major discrepancies between theory and experiment are more apparent for the singlet spectra than for the triplet.[2,3,5] We attribute these discrepancies mainly to autoionizing repulsive valence states and Rydberg states converging to excited ionic states. Perturbations of the resonant intermediate levels by repulsive valence states cannot be ignored; however, as discussed below, we expect this interaction to be of lesser consequence in the present REMPI problem.

1. Autoionization of repulsive valence states

Prior studies[2–5] of the photoionization of the O_2 $C\,^3\Pi_g$ Rydberg state have suggested the importance of autoionizing $^3\Delta_u$, $^3\Sigma_u^+$, and $^3\Sigma_u^-$ valence states derived from the $1\pi_u^3 1\pi_g^3$ electronic configuration. These repulsive states intersect the lower portion and rise above the potential energy curve of the $X\,^2\Pi_g$ ion, and may thus autoionize into the $^3\Delta_u$, $^3\Sigma_u^+$, and $^3\Sigma_u^-$ channels deriving from $3s\sigma_g \to k\pi_u$ ionization. To qualitatively discuss the importance of autoionization of these repulsive states, we introduce dimensionless autoionization probabilities $\zeta_{v^+}^2$ and the "survival factor" S ($S \leqslant 1$). The survival factor is the ratio between the dissociative recombination cross section and the capture cross section for a positive ion plus electron. Its departure from unity indicates the importance of autoionization compared with dissociation.[27] Following Giusti,[27] we define the quantities

$$\zeta_{v^+} = \pi \langle \chi_{v^+} | V(R) | \chi_d \rangle, \tag{2a}$$

$$V(R) = \langle \Phi_k | H | \Phi_d \rangle, \tag{2b}$$

$$S = \left[1 + \sum_{v^+} \zeta_{v^+}^2 \right]^{-2}, \tag{2c}$$

where χ_{v^+} and χ_d are vibrational wave functions of the ion and neutral dissociating state Φ_d, respectively, and H is the fixed-nuclei electronic Hamiltonian. Here Φ_k is the continuum wave function for $3s\sigma_g \to k\pi_u$ photoionization. We made Franck–Condon approximations to these quantities, i.e., $\zeta_{v^+} = \pi V(\bar{R}) \langle \chi_{v^+} | \chi_d \rangle$, where $\bar{R}$ is the centroid[28] $\bar{R} = \langle \chi_{v^+} | R | \chi_d \rangle / \langle \chi_{v^+} | \chi_d \rangle$. The differential Franck–Condon factors $\langle \chi_{v^+} | \chi_d \rangle$ were calculated using the $X\,^2\Pi_g$ curve of Krupenie[29] and the valence $^{1,3}\Sigma_u^-$, $^{1,3}\Sigma_u^+$, and $^{1,3}\Delta_u$ potential energy curves of Saxon and Liu[30] (shown in Fig. 1). The widths for the $^3\Sigma_u^-$, $^1\Delta_u$, and $^1\Sigma_u^+$ states calculated by Guberman[31] were employed, and we have assumed the triplet and singlet widths for states of the same spatial symmetry to be identical. The R-centroid procedure was employed

TABLE II. Autoionization probabilities and survival factors for singlet valence states.

$v'^{\rm a}$	v^+	$c\,^1\Sigma_u^-$	$1\,^1\Sigma_u^+$	$1\,^1\Delta_u$
0	0	5.0×10^{-3}	1.1×10^{-4}	6.7×10^{-2}
	1	3.3×10^{-2}	2.1×10^{-3}	0.21
		0.93[b]	1.0	0.61
1	0	2.8×10^{-3}	5.8×10^{-4}	0.11
	1	2.1×10^{-2}	8.3×10^{-3}	0.21
	2	6.7×10^{-2}	4.6×10^{-2}	2.6×10^{-2}
		0.84	0.90	0.55
2	0	1.5×10^{-3}	2.4×10^{-3}	0.16
	1	1.2×10^{-2}	2.5×10^{-2}	0.17
	2	4.5×10^{-2}	9.5×10^{-2}	2.1×10^{-3}
	3	9.5×10^{-2}	0.15	0.12
	4	0.12	6.8×10^{-2}	1.7×10^{-3}
		0.62	0.56	0.47
3	0	8.2×10^{-4}	6.9×10^{-2}	0.21
	1	7.4×10^{-3}	5.3×10^{-2}	9.5×10^{-2}
	2	3.0×10^{-2}	0.14	4.5×10^{-2}
	3	7.1×10^{-2}	0.11	8.4×10^{-2}
	4	0.11	2.7×10^{-3}	2.7×10^{-2}
	5	0.10	6.2×10^{-2}	6.5×10^{-2}
		0.57	0.48	0.43

[a] The single photon energy used in the (2 + 1) REMPI experiments of Ref. 14 for the $v'=0$–3 levels are 4.118, 4.230, 4.349, and 4.450 eV, respectively. The continuum vibrational energies for each repulsive state were obtained from the relation $E_c = 3\hbar\omega - [E(\infty) - \frac{1}{2}\hbar\omega_e]$, where $E(\infty)$ is the asymptotic energy with respect to the minimum of the $X\,^3\Sigma_g^-$ potential curve (Ref. 29), and ω_e is the ground-state vibrational frequency.

[b] Survival factors (see explanation in text).

only for the $^{1,3}\Sigma_u^-$ valence states, since widths for the other symmetries are essentially R independent.[31] In Tables II and III we give our calculated $\zeta_{v^+}^2$ matrix elements and survival factors for singlet and triplet valence states.

Focusing on the $v'=0$ level in Fig. 3, most of the observed intensity is concentrated in the $\Delta v = 0$ peak. The $\sim 10\%$ intensity in the $v^+=1$ peak likely derives from

TABLE III. Autoionization probabilities and survival factors for triplet valence states.

$v'^{\rm a}$	v^+	$B\,^3\Sigma_u^-$	$A\,^3\Sigma_u^+$	$C\,^3\Delta_u$
1	0	0.27	3.5×10^{-3}	3.9×10^{-3}
	1	0.20	2.0×10^{-2}	2.4×10^{-2}
	2	3.6×10^{-3}	4.8×10^{-2}	6.4×10^{-2}
		0.46[b]	0.87	0.84
2	0	0.20	2.0×10^{-3}	2.2×10^{-3}
	1	0.24	1.3×10^{-2}	1.5×10^{-2}
	2	1.4×10^{-2}	3.7×10^{-2}	4.7×10^{-2}
	3	9.6×10^{-2}	5.5×10^{-2}	7.9×10^{-2}
		0.42	0.82	0.77
3	0	0.14	1.2×10^{-3}	1.2×10^{-3}
	1	0.24	8.4×10^{-3}	9.6×10^{-3}
	2	6.8×10^{-2}	2.7×10^{-2}	3.3×10^{-2}
	3	2.5×10^{-2}	4.8×10^{-2}	6.6×10^{-2}
	4	0.14	4.9×10^{-2}	7.7×10^{-2}
	5	4.5×10^{-2}	2.3×10^{-2}	4.8×10^{-2}
		0.36	0.75	0.66

[a] The single-photon energy used in the (2 + 1) REMPI experiments of Ref. 2 for the $v'=1$–3 levels are 4.192, 4.306, and 4.418 eV, respectively.

[b] Survival factors (see explanation in text).

autoionization of the $^1\Delta_u$ valence state since its survival factor (Table II) deviates considerably from unity. Autoionization of the $^1\Delta_u$ state should remain prevalent for the $v'=1$ intermediate state.

Comparison with theory suggests that the $v'=2$ off-diagonal transitions have little contribution from direct ionization. At this level of excitation, the survival factor is about equal for all autoionizing states. Interestingly, there appears to be an effective partitioning of autoionization strength according to whether $\Delta v<0$ or $\Delta v>0$. Particularly for $\Delta v<0$ autoionization of the $^1\Delta_u$ state is strongest, while for $\Delta v>0$, $^1\Sigma_u^-$ and $^1\Sigma_u^+$ autoionization dominates.

For the $v'=3$ level again each symmetry makes a substantial contribution to autoionization. In Fig. 3 the apparent agreement between theory and experiment for the $v^+=4$ ionic level may be fortuitous since a theoretical treatment incorporating these autoionizing states will redistribute the photoelectron intensity. The increase of the parameter $\zeta^2_{v^+}$ for the $v^+=5$ ionic level relative to $v^+=4$ for $^1\Sigma_u^+$ and $^1\Delta_u$ symmetries may qualitatively account for the observed increase in photoelectron intensity.

It is interesting to compare the survival factors of the singlet autoionizing valence states with their triplet counterparts of Table III. With the exception of the $^3\Sigma_u^-$ state, autoionization of the singlet states appears more significant than in the triplet case. This circumstance supports the apparent poor level of agreement between present theory and experiment for the $d\,^1\Pi_g$ state. The large shift of the singlet valence states (compared to the triplets) results in overall more favorable Franck–Condon overlaps between the repulsive and ion potential curves.

The above qualitative analysis in terms of survival factors neglects interference with direct ionization. In fact, full theoretical consideration requires simultaneous treatment of the competing processes of direct ionization, autoionization, and dissociation. Such calculations have recently been achieved in REMPI studies[32,33] of the $C\,^1\Pi_u$ state of H_2. MQDT studies[34,35] of H_2 and NO have earlier considered a unified treatment of these competing processes in single-photon absorption. We are currently attempting to include these interactions in further studies of O_2.

2. Autoionization of Rydberg states converging to the $a\,^4\Pi_u$ and $A\,^2\Pi_u$ ionic states

Autoionizing states converging to the $a\,^4\Pi_u$ and $A\,^2\Pi_u$ states of O_2^+ have been investigated by many workers since the early work of Price and Collins,[36] and have recently been discussed and reviewed by Wu.[37] A high-resolution synchrotron study of autoionizing states converging to the $a\,^4\Pi_u$ ion has recently been reported,[38] as well as studies which prepare these states by charge-exchange translational spectroscopy.[39] The earlier discussions[1-5] of the $C\,^3\Pi_g$ REMPI-PES spectra neglected the possible role of these states. Their singlet analogs may influence the $d\,^1\Pi_g$ REMPI spectra as well. In Fig. 4 we show the relevant potential energy curves, and discuss qualitatively in the following section the role of these states in the $C\,^3\Pi_g$ and $d\,^1\Pi_g$ (2 + 1) REMPI problems.

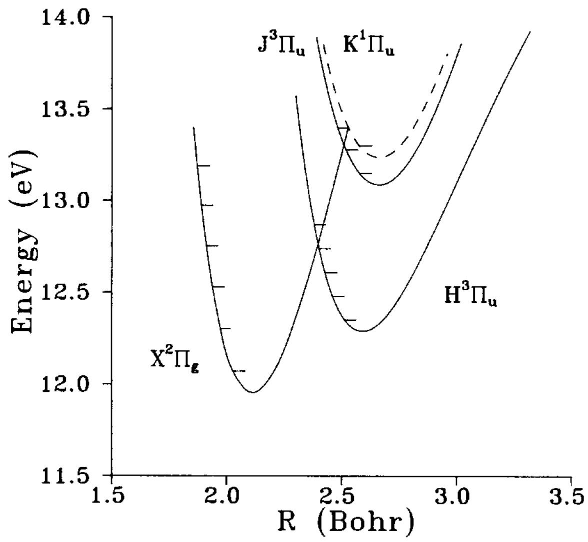

FIG. 4. Potential energy curves for the first ionic state, the $H\,^3\Pi_u$ ($1\pi_u^3 1\pi_g^2 3s\sigma_g$) Rydberg state converging to the $a\,^4\Pi_u$ ionic state (IP = 16.10 eV), and the $J\,^3\Pi_u$ and $K\,^1\Pi_u$ Rydberg states which converge to the $A\,^2\Pi_u$ ionic state (IP = 17.05 eV). The potentials for the H and J states are Morse curves constructed from constants given in Refs. 37 and 40. The K state (dashed curve) is shifted upward from the J state by 0.15 eV, as discussed in the text.

a. $^3\Pi_u$ autoionizing states. For triplet states, Nishitani *et al.*[40] have unambiguously assigned the vibrational progression in the 900–1010 Å region as all belonging to a single $H\,^3\Pi_u$ ($1\pi_u^3 1\pi_g^2 3s\sigma_g$) Rydberg state converging to the $a\,^4\Pi_u$ ion. This state is energetically accessible in the $v'=1$–3 levels of the $C\,^3\Pi_g$ one-color REMPI studies. Due to the large displacement of the potential curves, Franck–Condon factors become appreciable mainly for higher vibrational levels of the $X\,^2\Pi_g$ ion. Calculated Franck–Condon factors between the $H\,^3\Pi_u$ state and the $X\,^2\Pi_g$ ion are given in Table IV, which agree with the corresponding distributions plotted in Fig. 5 of Ref. 40. For one-color (2 + 1) REMPI via the $v'=1,2$ levels of the $C\,^3\Pi_g$ state, the total photon energy nearly coincides with the $v=2$($T_0=12.61$ eV) and $v=5$($T_0=12.98$ eV) levels of the $H\,^3\Pi_u$ state, respectively. Qualitatively, as follows from the theoretical analysis of

TABLE IV. Calculated Franck–Condon factors for the transitions O_2 $H\,^3\Pi_u(v)\rightarrow O_2^+$ $X\,^2\Pi_g(v^+)$.[a]

	$v=0$	1	2	3	4	5	6
$v^+=0$	0.0000	0.0002	0.0007	0.0019	0.0043	0.0080	0.0132
1	0.0003	0.0021	0.0069	0.0156	0.0280	0.0419	0.0543
2	0.0024	0.0117	0.0297	0.0520	0.0698	0.0755	0.0672
3	0.0104	0.0385	0.0716	0.0871	0.0746	0.0441	0.0149
4	0.0317	0.0825	0.0997	0.0672	0.0211	0.0002	0.0102
5	0.0718	0.1170	0.0715	0.0106	0.0046	0.0336	0.0477

[a] Franck–Condon factors were obtained using a Morse potential with spectroscopic constants from Ref. 40 for the O_2 $H\,^3\Pi_u$ state, and with the RKR potential of Ref. 29 for the O_2^+ $X\,^2\Pi_g$ state.

Smith[41] and Mies,[42] we would expect autoionization to be favored in the $\Delta v > 0$ transitions, i.e., the $v^+ = 2$ and 3 levels. These states could influence the vibrational distribution for the $v' = 3$ level of the $C\,^3\Pi_g$ state as well. Note that, although the Franck–Condon factors in Table IV are small, autoionization of the $H\,^3\Pi_u$ state is prominent in single-photon ionization spectra leading to the $X\,^2\Pi_g$ ion.[38,44]

The $J\,^3\Pi_u\,(1\pi_u^3 1\pi_g^2 3s\sigma_g)$ state, which is the first member of a Rydberg series converging to the $A\,^2\Pi_u$ ion,[37,40] lies 0.8 eV above the $H\,^3\Pi_u$ state and is energetically accessible in the $v' = 3$ REMPI spectra of the $C\,^3\Pi_g$ state. The total photon energy for $v' = 3$ (13.254 eV) lies slightly below the $v = 1$ level ($T_0 = 13.27$ eV) of the $J\,^3\Pi_u$ state. This level would preferentially autoionize into the $v^+ = 3$–5 levels of the ion, as qualitatively indicated by examining the $v = 1$ Franck–Condon distribution in Table IV, which should be nearly identical for the $J\,^3\Pi_u$ and $H\,^3\Pi_u$ states.

b. $^1\Pi_u$ autoionizing states. Singlet Rydberg states with the $1\pi_u^3 1\pi_g^2 3s\sigma_g$ configuration, which have not yet been observed, are likely relevant to one-color REMPI of the $d\,^1\Pi_g$ state. Such a singlet Rydberg state with the above configuration, which we denote $K\,^1\Pi_u$, may only be associated with the $A\,^2\Pi_u$ ion core, i.e., the singlet analog of the $J\,^3\Pi_u$ state (see Fig. 4). The predicted term value of $T_0 = 13.30$ eV (derived below) makes this state energetically accessible for the $v' = 3$ REMPI spectra of the $d\,^1\Pi_g$ state (Fig. 3). In particular, the total photon energy for the $v' = 3$ $d\,^1\Pi_g$ state REMPI spectra (13.380 eV) nearly coincides with the $v = 0$ level of the $K\,^1\Pi_u$ state. Therefore, from Table IV (which should remain essentially valid for the $K\,^1\Pi_u$ state) we expect preferential autoionization into $v^+ = 3$–5 levels of the ion.

c. SCF calculations. To support the above qualitative discussion and previous assignments of the H and $J\,^3\Pi_u$ states,[37,40] we have performed single-configuration SCF calculations on the J, H, and the $K\,^1\Pi_u$ state of O_2. The open-shell wave functions for these states have the form

$$\begin{aligned}\Psi(H\,^3\Pi_u) = \frac{1}{\sqrt{12}}\{3&|1\pi_u^+\,\overline{1\pi_u}^+\,1\pi_u^-\,\overline{3s\sigma_g}\,1\pi_g^+\,1\pi_g^-|\\ &-|1\pi_u^+\,\overline{1\pi_u}^+\,\overline{1\pi_u}^-\,3s\sigma_g\,1\pi_g^+\,1\pi_g^-|\\ &-|1\pi_u^+\,\overline{1\pi_u}^+\,1\pi_u^-\,3s\sigma_g\,\overline{1\pi_g}^+\,1\pi_g^-|\\ &-|1\pi_u^+\,\overline{1\pi_u}^+\,1\pi_u^-\,3s\sigma_g\,1\pi_g^+\,\overline{1\pi_g}^-|\},\end{aligned} \tag{3a}$$

$$\begin{aligned}\Psi(J\,^3\Pi_u) = \frac{1}{\sqrt{6}}\{2&|1\pi_u^+\,\overline{1\pi_u}^+\,\overline{1\pi_u}^-\,3s\sigma_g\,1\pi_g^+\,1\pi_g^-|\\ &-|1\pi_u^+\,\overline{1\pi_u}^+\,1\pi_u^-\,3s\sigma_g\,1\pi_g^+\,\overline{1\pi_g}^-|\\ &-|1\pi_u^+\,\overline{1\pi_u}^+\,1\pi_u^-\,3s\sigma_g\,\overline{1\pi_g}^+\,1\pi_g^-|\},\end{aligned} \tag{3b}$$

$$\begin{aligned}\Psi(K\,^1\Pi_u) = \frac{1}{\sqrt{12}}\{2&|1\pi_u^+\,\overline{1\pi_u}^+\,1\pi_u^-\,3s\sigma_g\,\overline{1\pi_g}^+\,\overline{1\pi_g}^-|\\ &-|1\pi_u^+\,\overline{1\pi_u}^+\,\overline{1\pi_u}^-\,3s\sigma_g\,1\pi_g^+\,\overline{1\pi_g}^-|\\ &-|1\pi_u^+\,\overline{1\pi_u}^+\,\overline{1\pi_u}^-\,3s\sigma_g\,\overline{1\pi_g}^+\,1\pi_g^-|\\ &+2|1\pi_u^+\,\overline{1\pi_u}^+\,\overline{1\pi_u}^-\,\overline{3s\sigma_g}\,1\pi_g^+\,1\pi_g^-|\\ &-|1\pi_u^+\,\overline{1\pi_u}^+\,1\pi_u^-\,\overline{3s\sigma_g}\,1\pi_g^+\,\overline{1\pi_g}^-|\\ &-|1\pi_u^+\,\overline{1\pi_u}^+\,1\pi_u^-\,\overline{3s\sigma_g}\,\overline{1\pi_g}^+\,1\pi_g^-|\}.\end{aligned} \tag{3c}$$

With a basis identical to that of the $C\,^3\Pi_g$ and $d\,^1\Pi_g$ state SCF calculations, we find total energies of $-149.240\,43$, $-148.875\,84$, and $-148.870\,34$ a.u., at $R = 2.282\ a_0$, respectively, for these states. For the $H\,^3\Pi_u$ state, we calculate the $3s\sigma_g$ orbital eigenvalue to be -3.52 eV. Using the experimental ionization potential of 16.10 eV,[37,40] we calculate a term value and quantum defect of $T_0 = 12.58$ eV and $\delta = 1.034$, which compare reasonably well with the experimental values[40] of 12.35 eV and 1.095, respectively. The $J\,^3\Pi_u$ and $K\,^1\Pi_u$ states each consist of a mixture between three components, corresponding to the three parentages $^3\Sigma_g^-$, $^1\Delta_g$ and $^1\Sigma_g^+$ associated with the $^2\Pi_u\,(1\pi_u^3 1\pi_g^2)$ states of the ion core.[45,46] Instead of solving a three term secular problem, we invoke a simplification by initially calculating the $J\,^3\Pi_u$ and $K\,^1\Pi_u$ SCF states corresponding to pure $^3\Sigma_g^-$ parentage. The wave functions given in Eqs. (3b) and (3c) above assume this single parentage. We then calculated an empirically corrected term value for the $J\,^3\Pi_u$ state by employing the $3s\sigma_g$ orbital eigenvalue, -3.67 eV, and the observed $A\,^2\Pi_u$ ionization potential, 17.05 eV.[37,40] For the $J\,^3\Pi_u$ state our calculation gives $T_0 = 13.38$ eV and $\delta = 1.075$, compared to the experimental values[40] of 13.15 eV and 1.133, respectively. Using the singlet–triplet splitting obtained by subtracting total $J\,^3\Pi_u$ and $K\,^1\Pi_u$ SCF energies (0.15 eV), and the *experimental* term value of the $J\,^3\Pi_u$ state, the predicted term value of the $K\,^1\Pi_u$ state is $T_0 = 13.30$ eV, with a singlet quantum defect of $\delta = 1.095$.

The $^{1,3}\Pi_u$ Rydberg states may be incorporated into *ab initio* photoionization calculations using the Smith–Mies–Fano[41–43] procedure or an appropriate MQDT treatment. However since the $^{1,3}\Pi_u$ ionization channels contain the σ_u shape resonance, the associated non-Franck–Condon effect must be incorporated explicitly, as done here at the one-electron level for direct photoionization.

3. Initial-state perturbations

Another mechanism leading to non-Franck–Condon effects in vibrational distributions is perturbation of the initial Rydberg state by the valence–Rydberg interaction, i.e., an avoided crossing. The $C\,^3\Pi_g$ and $d\,^1\Pi_g$ Rydberg states of O_2 are intersected by $1\,^3\Pi_g$ and $1\,^1\Pi_g$ valence potential energy curves, which are derived from the electronic configuration $3\sigma_g 1\pi_g^3$. Cartwright *et al.*[8] first postulated the weak electronic interaction leading to the interpretation of two crossing diabatic states near the minimum of the $C\,^3\Pi_g$ Rydberg potential curve. For the $d\,^1\Pi_g$ state, Van der Zande *et al.*[16] have recently deduced the coupling matrix element H_{el} of 55 meV from their kinetic-energy-release spectra, and accounted for the decrease in rotational constant $B_{v'}$ going from $v' = 0$–3, and its return to that of the ion for $v' > 3$. To estimate the effect of this perturbation on the $d\,^1\Pi_g$ REMPI spectra, we calculated the $v' = 0$–3 vibrational wave functions for the lower adiabatic potential ($v' = 1,4,8,12$ for the double well[16]) without nonadiabatic coupling, and directly incorporated them in the calculation of the vibrational branching ratios. Since a dipole transition between the $3\sigma_g 1\pi_g^3$ state and the $3s\sigma_g \rightarrow k\pi_u$ continuum is very weak, and nonadiabatic corrections to the vibrational wave functions are small,[16] we expect this procedure to be a good approximation. We found almost negligible changes in the branching ratios, due to the preservation of nodal structure of the vibrational wave functions in the inner region of the double-well potential curve. This further indicates that the (final-state) autoionization effects discussed above are likely dominant. For situations where there is a strong avoided crossing, e.g., the $B\,^3\Sigma_u^- - E\,^3\Sigma_u^-$ system of O_2, one must solve the coupled Schrödinger equations for a full treatment.[47,48]

C. Photoelectron angular distributions

Figure 5 shows calculated vibrationally resolved photoelectron angular distributions for the $v' = 0$ and 1 levels of the $d\,^1\Pi_g$ Rydberg state. In these figures we have plotted the angular distribution

$$\frac{d\sigma}{d\Omega} \propto 1 + \beta P_2(\cos\theta), \tag{4}$$

where β is the asymmetry parameter for an unaligned molecular target, θ is the angle between the direction of the light polarization and the photoelectron momentum, and P_2 is a Legendre polynomial. The numerical values of the β parameters and those for other v' levels are given in Table V. No experimental values are available for the $d\,^1\Pi_g$ state, although a comparision between theory and experimental results for the $C\,^3\Pi_g$ state has been made, with satisfying results.[4,5] Note that we have neglected any effects due to state alignment arising from the two-photon excitation. This will be of interest in future experimental studies of specific rotational branches.

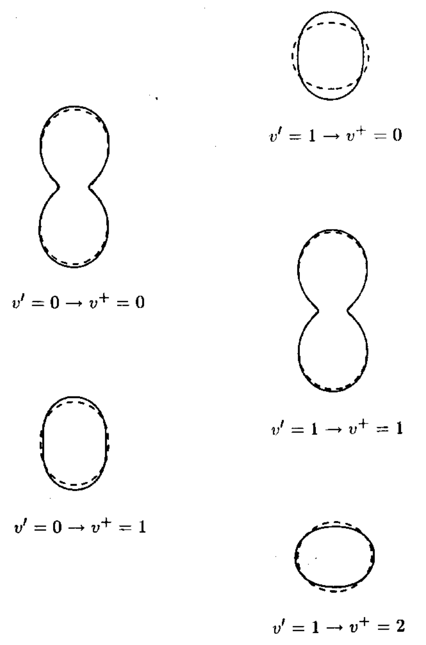

FIG. 5. Calculated photoelectron angular distributions for the $v' = 0$ and 1 levels of the O_2 $d\,^1\Pi_g$ state. Solid curve: length form; dash curve: velocity form. In this figure $\theta = 0$ is vertical.

TABLE V. Summary of calculated vibrationally resolved asymmetry parameters.

v'	v^+	β_{v',v^+}	
		Length	Velocity
0	0	1.213	1.126
0	1	0.282	0.143
1	0	0.202	−0.086
1	1	1.227	1.162
1	2	−0.150	−0.027
2	0	0.572	0.591
2	1	−0.181	−0.110
2	2	1.232	1.201
2	3	0.013	−0.092
2	4	0.790	0.660
3	0	0.121	0.128
3	1	0.448	0.445
3	2	0.002	0.086
3	3	1.240	1.278
3	4	0.335	0.098
3	5	0.683	0.583

The difference between $\Delta v = 0$ and $\Delta v \neq 0$ distributions is very large, due to the non-Franck–Condon effect associated with the σ_u resonance. This is similar to that discussed for the $C\,^3\Pi_g$ state.[5] However, there is also considerable difference between the $\Delta v \neq 0$ angular distributions for the singlet state compared to the triplet. For example, for the $v' = 1 \rightarrow v^+ = 2$ transition, the calculated[5] (velocity form) β for the triplet state is 0.55, and $\beta = -0.027$ for the singlet (Table V), at nearly the same total photon energy of ~ 12.5 eV.

It would be interesting to experimentally measure these photoelectron angular distributions to confirm this large multiplet-specific effect, which is not too apparent when comparing the singlet and triplet branching ratios. Additionally, it would be useful to measure changes in the higher-order terms in the REMPI angular distributions and compare them with their triplet counterparts[4,5] so as to ascertain the role of spin coupling in the alignment induced by the two-photon absorption step.

D. Energy-dependent branching ratios and angular distributions

$(2 + 1')$ two-color REMPI studies of the $d\,^1\Pi_g$ state may provide useful insight into the role of autoionization on these ion vibrational distributions. To illustrate what the present one-electron theory predicts for the energy dependence of such distributions, Fig. 6 shows calculated vibrationally resolved branching ratios and photoelectron angular distributions for photoionization of the $v' = 3$ level over a range of photon energies. For the branching ratios, all curves begin at 4.32 eV photon energy above the $v' = 3$ level of the $d\,^1\Pi_g$ state and the $v^+ = 0$–5 channels are hence energeti-

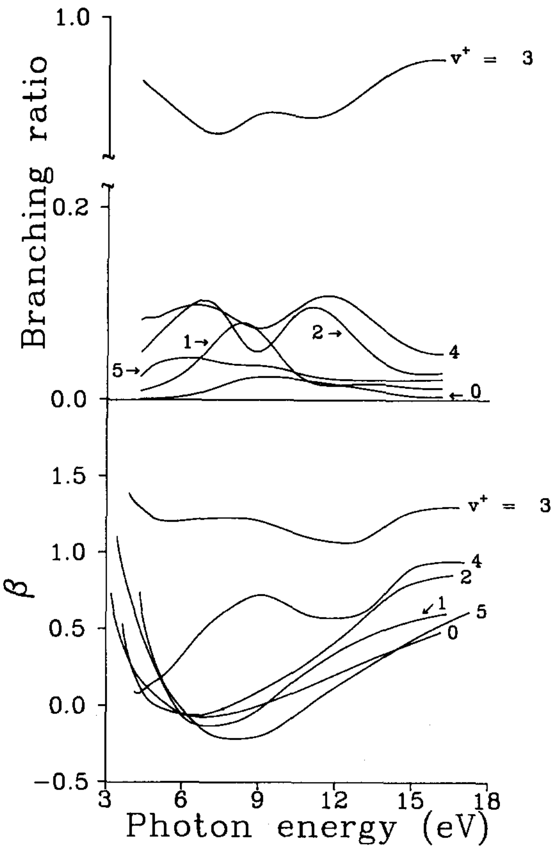

FIG. 6. Calculated energy-dependent vibrational branching ratios and asymmetry parameters for the $v' = 3$ level of the O_2 $d\,^1\Pi_g$ state leading to the $v^+ = 0$–5 levels of the ion.

cally open. The distributions are normalized such that a sum at any photon energy equals unity.

The $\Delta v = 0$ component dominates at all photon energies. For $\Delta v \neq 0$ distributions, the $v' = 3 \rightarrow v^+ = 4$ ratio is the dominant component, due to strong asymmetry of the R-dependent amplitudes at larger internuclear distances where the shape resonance is most intense. Due to nodal structure of the vibrationally excited initial state wave functions, secondary maxima associated with the resonance may occur in the cross sections (and thus branching ratios), e.g., ~ 11 eV photon energy. Thus, we predict an apparent "detuning" effect from the resonance to occur near threshold, e.g., ~ 9 eV for the $v' = 3 \rightarrow v^+ = 2$–4 ratios, and at photon energies beyond 15 eV for all transitions.

The strong variation in asymmetry parameter β with v^+ in the bottom of Fig. 6 reflects the non-Franck–Condon effect induced by the shape resonance, as seen previously in angular distribution studies of O_2 $C\,^3\Pi_g$ photoionization,[4,5] and other studies of molecules in their ground state.[25] The structure in the $v^+ = 3$ and 4 distributions reflects the secondary maxima occuring in the vibrational branching ratios.

IV. CONCLUSION

We have presented ionic vibrational branching ratios and vibrationally resolved photoelectron angular distributions for photoionization of the $d\,^1\Pi_g$ Rydberg state of O_2. The non-Franck–Condon effects induced by the σ_u shape resonance accounts for some of the observed[14] deviations from the expected $\Delta v = 0$ propensity rule for ionization of molecular Rydberg states. However, the vibrational branching ratios calculated with the Hartree–Fock model, which include the effects of the shape resonance, differ significantly from the observed values. There are no measurements of the photoelectron angular distributions for the $d\,^1\Pi_g$ state. It would be interesting to compare these photoelectron angular distributions with those for the $C\,^3\Pi_g$ state,[4] since the present calculations predict significant differences due to the particular spin couplings in the resonant intermediate and final states.

In the present $d\,^1\Pi_g$ REMPI problem, multichannel interactions involving both repulsive and Rydberg autoionizing states likely result in the major departures from the simple Franck–Condon prediction. We have tentatively identified these interactions as arising from autoionization of singlet valence states derived from the $1\pi_u^3 1\pi_g^3$ electronic configuration, analogous to earlier assessments for the $C\,^3\Pi_g$ state.[2–5] Evidence has also been presented which indicates that Rydberg states which converge to the $a\,^4\Pi_u$ and $A\,^2\Pi_u$ ion states may be responsible for a portion of the observed $\Delta v \neq 0$ intensity, in both $C\,^3\Pi_g$ and $d\,^1\Pi_g$ state REMPI spectra. Since the singlet states associated with the $A\,^2\Pi_u$ ion core have not been observed, it may be of interest to probe them directly by inducing single-photon transitions from, e.g., the O_2 $X\,^3\Sigma_g^-$ or $^1\Delta_g$ states, or by charge-exchange translational spectroscopy.

ACKNOWLEDGMENTS

The authors are grateful to P. J. Miller and W. A. Chupka for permission to use unpublished REMPI photoelectron spectra for the O_2 $d\,^1\Pi_g$ state in this work. This work was supported by grants from the National Science Foundation (CHE-8521391), Air Force Office of Scientific Research (Contract No. 87-0039), and the Office of Health and Environmental Research of the U.S. Department of Energy (DE-FG03-87ER60513). We also acknowledge use of resources of the San Diego SuperComputer Center, which is supported by the National Science Foundation. One of us (M. B.) would like to acknowledge support from a Department of Education Fellowship.

[1] S. Katsumata, K. Sato, Y. Achiba, and K. Kimura, J. Electron Spectrosc. Relat. Phenom. **41**, 325 (1986).
[2] P. J. Miller, L. Li, W. A. Chupka, and S. D. Colson, J. Chem. Phys. **89**, 3921 (1988).
[3] J. A. Stephens, M. Braunstein, and V. McKoy, J. Chem. Phys. **89**, 3923 (1988).
[4] P. J. Miller, W. A. Chupka, J. Winniczek, and M. G. White, J. Chem. Phys. **89**, 4058 (1988).
[5] M. Braunstein, J. A. Stephens, and V. McKoy J. Chem. Phys. **90**, 633 (1989).
[6] H. Park, P. J. Miller, W. A. Chupka, and S. D. Colson, J. Chem. Phys. **89**, 3919 (1988).
[7] H. Park, P. J. Miller, W. A. Chupka, and S. D. Colson, J. Chem. Phys. **89**, 6676 (1988).

[8] D. C. Cartwright, W. J. Hunt, W. Williams, S. Trajmar, and W. A. Goddard, Phys. Rev. A **8**, 2436 (1973).
[9] S. Trajmar, D. C. Cartwright, and R. I Hall, J. Chem. Phys. **65**, 5275 (1976).
[10] T. York and J. Comer, J. Phys. B **16**, 3627 (1983).
[11] A. Sur, C. V. Ramana, and S. D. Colson, J. Chem. Phys. **83**, 904 (1985).
[12] A. Sur, C. V. Ramana, W. A. Chupka, and S. D. Colson, J. Chem. Phys. **84**, 904 (1985).
[13] R. D. Johnson, G. R. Long, and J. W. Hudges, J. Chem. Phys. **87**, 1977 (1987).
[14] P. J. Miller and W. A. Chupka (private communication).
[15] W. J. van der Zande, W. Koot, J. R. Peterson, and J. Los, Chem. Phys. Lett. **140**, 175 (1987).
[16] W. J. van der Zande, W. Koot, J. Los, and J. R. Peterson, J. Chem. Phys. **89**, 6758 (1988).
[17] R. R. Lucchese, G. Raseev, and V. McKoy, Phys. Rev. A **25**, 2572 (1982).
[18] R. R. Lucchese, K. Takatsuka, and V. McKoy, Phys. Rep. **131**, 147 (1986), and references therein.
[19] G. Raseev, H. Lefebvre-Brion, H. LeRouzo, and A. L. Roche, J. Chem. Phys. **74**, 6686 (1981).
[20] A. Gerwer, C. Asaro, B. V. McKoy, and P. W. Langhoff, J. Chem. Phys. **72**, 713 (1980).
[21] P. M. Dittman, D. Dill, and J. L. Dehmer, J. Chem. Phys. **76**, 5703 (1982).
[22] M. Braunstein and V. McKoy, J. Chem. Phys. **90**, 2575 (1989).
[23] M. Braunstein, V. McKoy, and M. E. Smith, J. Chem. Phys. **90**, 3931 (1989).
[24] J. L. Dehmer, D. Dill, and S. Wallace, Phys. Rev. Lett. **43**, 1005 (1979); R. Stockbauer, B. E. Cole, D. L. Ederer, J. B. West, A. C. Parr, and J. L. Dehmer, *ibid.* **43**, 757 (1979); J. B. West, A. C. Parr, B. E. Cole, D. L. Ederer, R. Stockbauer, and J. L. Dehmer, J. Phys. B **13**, 1105 (1980).
[25] J. L. Dehmer, A. C. Parr, and S. H. Southworth, in *Handbook on Synchrotron Radiation*, edited by G. V. Marr (North-Holland, Amsterdam, 1987), Vol. II, p. 241.
[26] I. Nenner and J. A. Beswick, in *Handbook on Synchrotron Radiation*, edited by G. V. Marr (North-Holland, Amsterdam, 1987). Vol. II, p. 355.
[27] A. Giusti, J. Phys. B **13**, 3867 (1980).
[28] H. Lefebvre-Brion and R. W. Field, *Pertubations in the Spectra of Diatomic Molecules* (Academic, Orlando, 1986), Chap. 2, Sec. 3.1.
[29] P. Krupenie, J. Phys. Chem. Ref. Data **1**, 423 (1972).
[30] R. P. Saxon and B. Liu, J. Chem. Phys. **67**, 5432 (1977).
[31] S. L. Guberman, Planet. Space Sci. **36**, 47 (1988).
[32] S. N. Dixit, D. L. Lynch, V. McKoy, and A. U. Hazi, Phys. Rev. A **40**, 1700 (1989).
[33] A. P. Hickman, Phys. Rev. Lett. **59**, 1553 (1987).
[34] Ch. Jungen, Phys. Rev. Lett. **53**, 2394 (1984).
[35] A. Giusti-Suzor and Ch. Jungen, J. Chem. Phys. **80**, 986 (1984).
[36] W. C. Price and G. Collins, Phys. Rev. **48**, 714 (1935).
[37] C. Y. Wu, J. Quant. Spectrosc. Radiat. Transfer **37**, 1 (1987).
[38] D. M. P. Holland and J. B. West, Z. Phys. D **4**, 367 (1987).
[39] W. J. van der Zande, W. Koot, J. R. Peterson, and J. Los, Chem. Phys. **126**, 169 (1988).
[40] E. Nishitani, I. Tanaka, K. Tanaka, T. Kato, and I. Koyano, J. Chem. Phys. **81**, 3429 (1984).
[41] A. L. Smith, Philos. Trans. R. Soc. London Ser A **268**, 169 (1970); J. A. Kinsinger and J. W. Taylor, Int. J. Mass Spectrosc. Ion Phys. **11**, 461 (1973). See also Ref. 26, Sec. 3.2.3.
[42] F. H. Mies, Phys. Rev. **175**, 164 (1968).
[43] U. Fano, Phys. Rev. **124**, 1866 (1961).
[44] P. M. Dehmer and W. A. Chupka, J. Chem. Phys. **62**, 4525 (1975).
[45] R. N. Dixon and S. E. Hull, Chem. Phys. Lett. **3**, 367 (1969); See also Ref. 28, Sec. 2.2.3 for a thorough discussion of this problem.
[46] N. Honjou, K. Tanaka, K. Ohno, and H. Taketa, Mol. Phys. **35**, 1569 (1978).
[47] J. Wang, A. J. Blake, and L. Torop, J. Chem. Phys. **89**, 4654 (1988).
[48] P. J. Miller, L. Li, W. A. Chupka, and S. D. Colson, J. Chem. Phys. **88**, 2972 (1988).